

## Forcing the Climate Fraud

Roy Clark PhD

### Ventura Photonics Climate Note 3, VPCN 003.1

Ventura Photonics

Thousand Oaks

September 2019

The calculation of the local surface temperature of the earth requires a detailed engineering analysis of the various energy transfer processes involved. The time dependent heating and cooling flux terms are coupled to the local surface thermal reservoir. The change in temperature over a given time period is determined by the change in heat content or enthalpy of this reservoir divided by its heat capacity. The energy transfer properties of the land-air and the ocean-air interfaces are different and have to be considered separately. To complicate matters, the weather station temperature is not the surface temperature. Instead it is the meteorological surface air temperature (MSAT) measured in a ventilated enclosure located 1.5 to 2 m above the ground. Any change in surface temperature then has to be converted into a change in MSAT. The minimum and maximum MSATs are produced by different energy transfer processes and both have to be calculated to determine the average. When the time dependence is explicitly included in the calculation, there is another important parameter that needs to be considered. This is the time delay or phase shift between the solar flux and the temperature response. There is both a diurnal and a seasonal phase shift that should be correctly predicted by the thermal analysis. This is discussed in detail by Clark [2019a].

All of this has been conveniently ignored in the climate models. Physical reality has been abandoned in favor of mathematical simplicity. Instead of performing a thermal engineering calculation to determine the surface temperature, a prescribed mathematical ritual known as radiative forcing is used. It is assumed that a change in surface temperature  $\Delta T$  can be associated with a change in LWIR flux at the top of the atmosphere that in turn is related to a change in atmospheric concentration of 'greenhouse gas' (or aerosol).

$$\Delta T = \lambda RF \quad (\text{Eq. 1})$$

Where  $\lambda$  is a ‘climate sensitivity constant’ and RF is the radiative forcing or change in LWIR flux [Harde, 2017; 2013]. The mathematical ritual for calculating the change in temperature is illustrated in Figure 1 [IPCC Ch.8, 2013; Hansen et al, 2005; 1981].

First, a ‘before’ and ‘after’ radiative transfer calculation is performed to determine the change in LWIR flux produced by the change in atmospheric concentration of the ‘forcing agent’ of interest. Typically this has involved a doubling of the CO<sub>2</sub> concentration. This is called the ‘instantaneous’ radiative forcing. The stratosphere is then allowed to ‘adjust’ to create a new ‘equilibrium state’. The ‘stratospherically adjusted’ radiative forcing is then used to ‘adjust’ the atmospheric temperature profile with the surface temperature fixed, the land surface temperature is then allowed to ‘adjust’ and finally the whole coupled model climate system is allowed to adjust. This is supposed to give some kind of ‘equilibrium’ forcing response in which the oceans ‘adjust’ to a new temperature.

Using this approach, the ‘radiative forcings’ that can be attributed to changes in the atmospheric concentration of various ‘greenhouse gases’ and other ‘forcing agents’ can be calculated. At least for the ‘greenhouse gases’ the underlying radiative transfer calculations of the LWIR flux changes should be reliable. These are derived from HITRAN data that has been compiled independently of any climate ‘science’. However, there is simply no connection between the calculated ‘forcings’ and any change in surface temperature. Radiative forcing is empirical pseudoscience or climate astrology. The ‘forcings’ published by the IPCC in their 2013 AR5 report are illustrated in Figure 2 [IPCC, 2013, Ch. 8].

In order to understand the fraud associated with radiative forcing it is necessary to consider three separate aspects of the climate energy transfer. First, there is no equilibrium to adjust in the outgoing longwave radiation (OLR) emitted to space. Second, the downward flux from the stratosphere and upper troposphere cannot couple to the surface because of molecular linewidth effects and third, the downward LWIR flux at the surface cannot couple to the surface thermal reservoirs in a way that can cause any measurable change in surface temperature. This also means that there can be no CO<sub>2</sub> ‘signature’ in the weather station record. These three areas will now be considered in more detail.

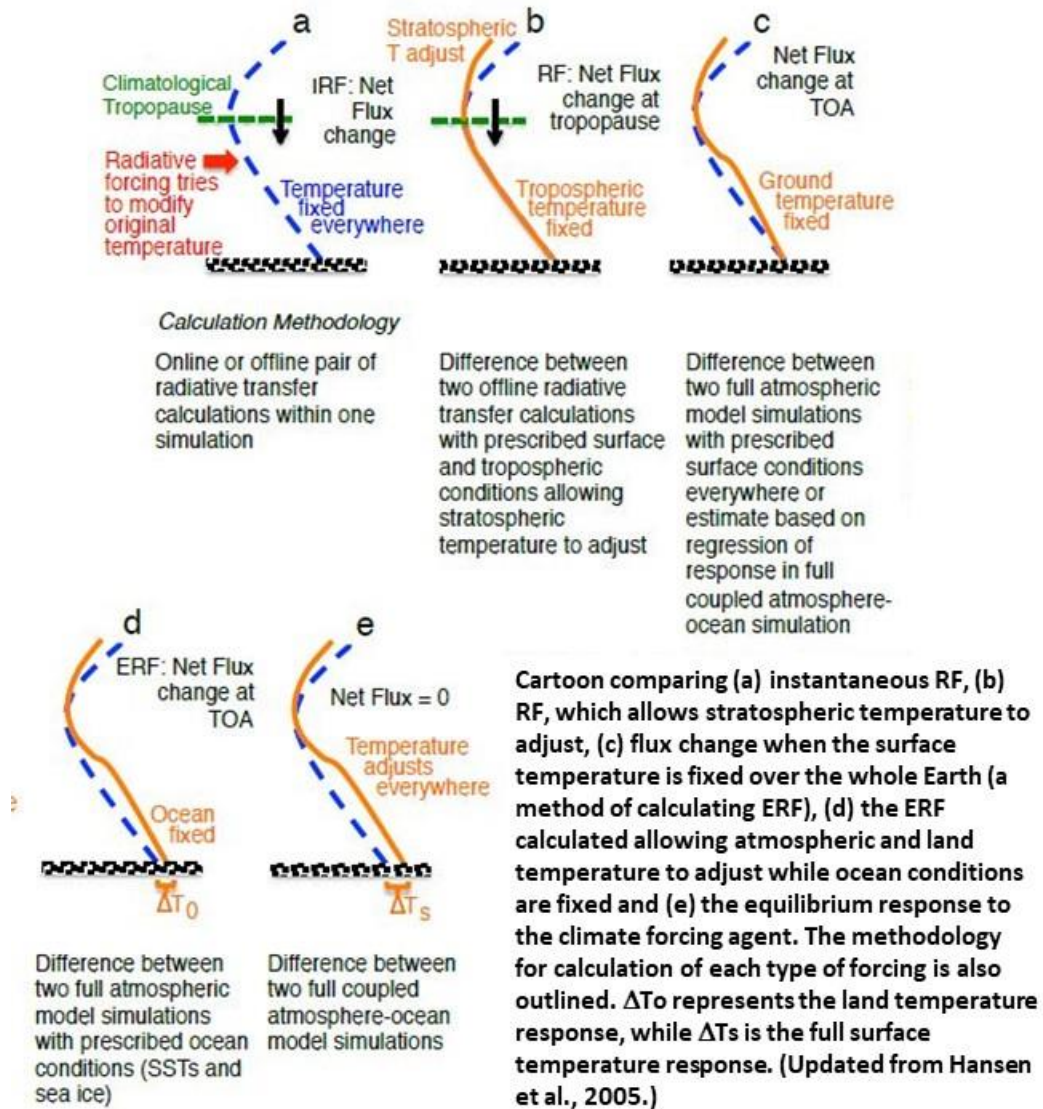


Figure 1: Climate model adjustments to determine the change in temperature of the climate system from an input ‘radiative forcing’ [IPCC, 2013, Ch. 8].

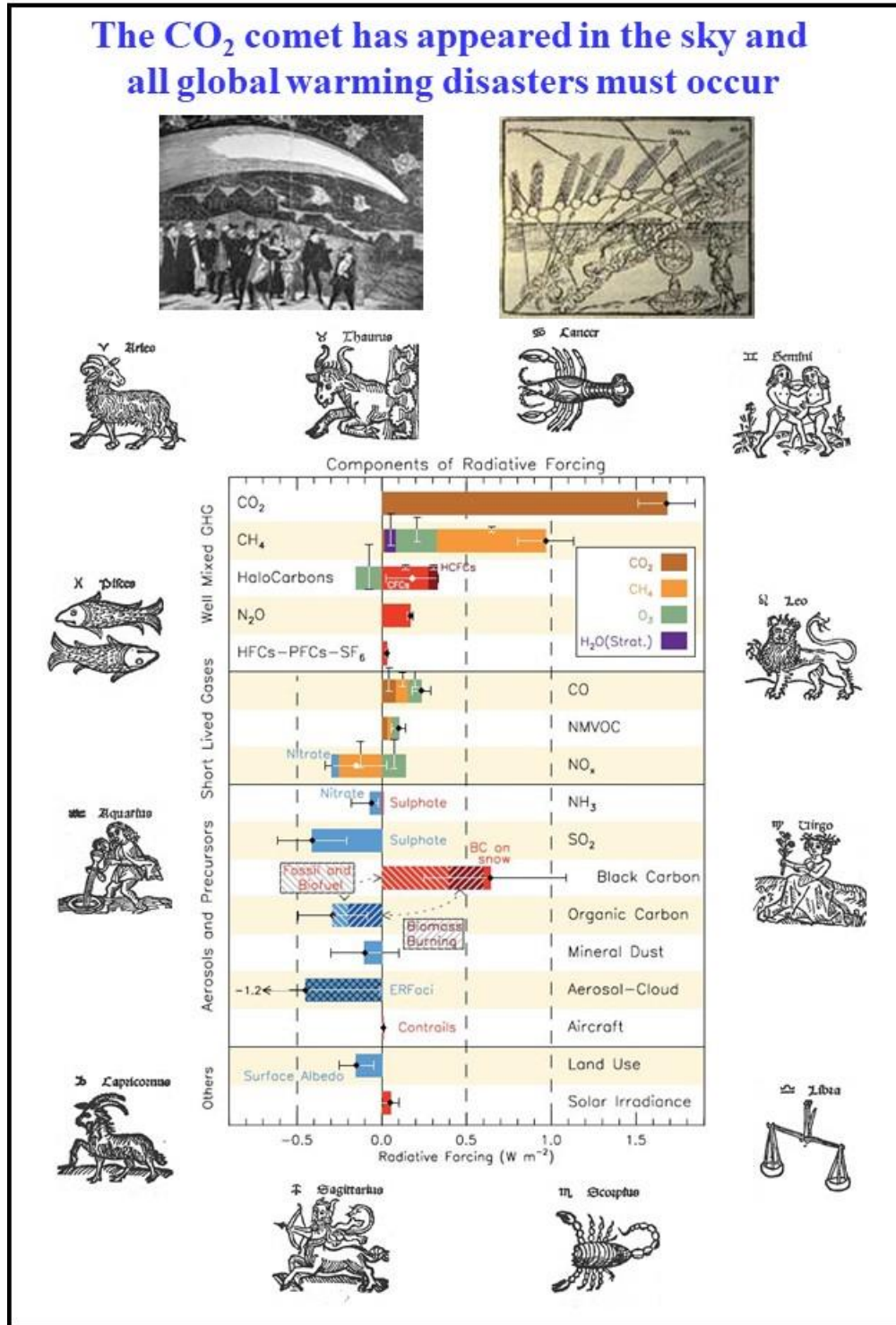
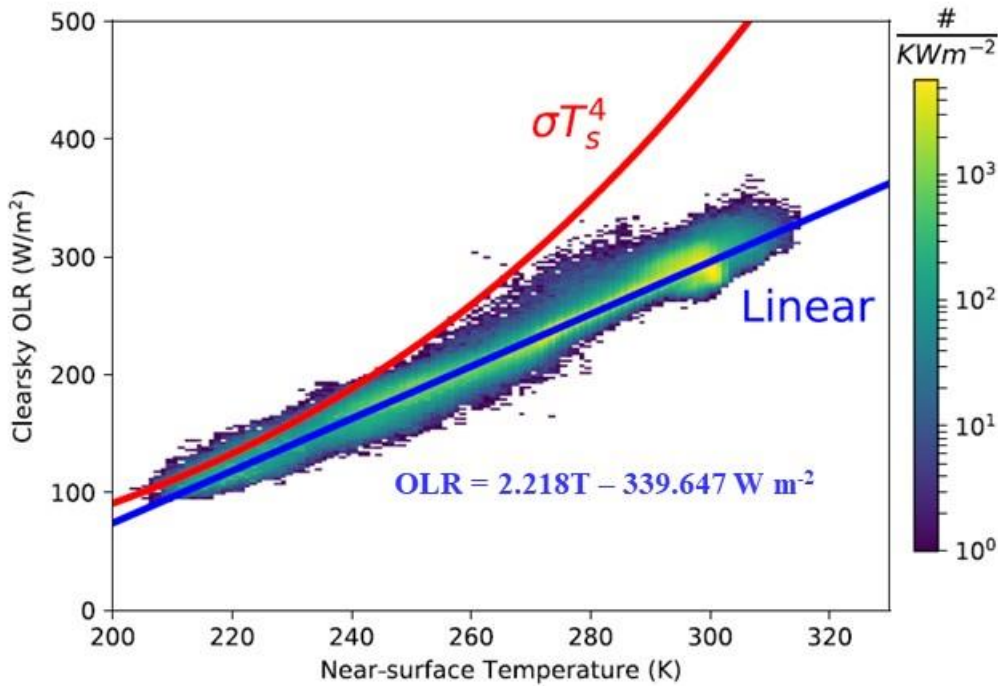


Figure 2: Radiative forcing constants from the IPCC AR5 report

## The OLR Emitted to Space

It has long been known that an increase in surface temperature produces an increase in the OLR emitted to space and that the (cloud free) OLR response is approximately linear in temperature. This temperature response is shown in Figure 3 [Koll and Cronin, 2018]. This is discussed in detail by Clark [2019d]



**Figure 3: Linear dependence of OLR emission on near surface temperature [From Koll and Cronin, 2018]**

Figure 4 shows the spectral distribution for the OLR for a surface and surface air temperature of 300 K at 70% surface relative humidity (RH). The spectral range is from 100 to 1500  $\text{cm}^{-1}$  at a resolution of 2  $\text{cm}^{-1}$ . These spectra are from MODTRAN calculations using the default tropical atmosphere with a  $\text{CO}_2$  concentration of 400 ppm [MODTRAN, 2018]. Starting from left to right, the main spectral features are the rotational  $\text{H}_2\text{O}$  band from 100 to 600  $\text{cm}^{-1}$ , the  $\text{CO}_2$   $\nu_2$  vibration band from 600 to 750  $\text{cm}^{-1}$  and the  $\text{H}_2\text{O}$   $\nu_2$  vibration band above 1300  $\text{cm}^{-1}$  [Herzberg, 1991]. P and R denote the  $\text{CO}_2$  band structure associated with the P ( $\Delta J = -1$ ) and R ( $\Delta J = +1$ ) rotational transitions. Between 750 and 1250  $\text{cm}^{-1}$  there is a spectral transmission window that consists of weak  $\text{H}_2\text{O}$  lines and two  $\text{CO}_2$  overtone bands near 950 and 1050  $\text{cm}^{-1}$ . This allows some of the blackbody emission from the surface to be transmitted directly to space. There is also an absorption feature from stratospheric ozone,  $\text{O}_3$  that occurs near 1050  $\text{cm}^{-1}$  in the OLR emission. The OLR is for 70 km looking down. For reference, blackbody emission curves for 300 to 220 K in 20 K intervals are also plotted. The calculated MODTRAN 300 K blackbody emission from the surface is also shown (MODTRAN, 0 km looking down).

Figure 5 shows the OLR flux from Figure 4 divided into the separate atmospheric and surface emission contributions. Assuming a lapse rate near  $6.5 \text{ K km}^{-1}$ , each 20 K decrease in temperature corresponds approximately to a 3 km increase in altitude. In the  $500$  to  $600 \text{ cm}^{-1}$  region, the  $\text{H}_2\text{O}$  emission is from an altitude of  $\sim 4.5 \text{ km}$  at a temperature of  $\sim 270 \text{ K}$ . Near  $300 \text{ cm}^{-1}$  the  $\text{H}_2\text{O}$  emission temperature has decreased to  $\sim 240 \text{ K}$  at an altitude of  $\sim 9 \text{ km}$ . However, the emission temperature of the main  $\text{CO}_2$  P and R bands is  $\sim 220 \text{ K}$  indicating that the absorption and emission process continues through the troposphere and into the stratosphere [Clark, 2019c].

There are two different contributions to the temperature dependence of the OLR flux. Within the main  $\text{H}_2\text{O}$  and  $\text{CO}_2$  absorption bands, the OLR emission does not change significantly with surface temperature. The absorption and emission process continues with increasing altitude until the molecular linewidths narrow sufficiently to allow the transition to a free photon flux to space. For  $\text{H}_2\text{O}$ , this transition occurs near a temperature of  $253 \text{ K}$  ( $-20 \text{ C}$ ). As the surface temperature changes, the altitude of the  $\text{H}_2\text{O}$  emission band changes. For  $\text{CO}_2$  the free photon transition occurs at a lower temperature near  $220 \text{ K}$ . Most of the  $\text{CO}_2$  band emission occurs in the stratosphere. The spectral band cooling rates vs altitude for a tropical atmosphere are shown in Figure 6 [Feldman et al, 2008]. The linear temperature dependence comes from the flux emitted in the spectral transmission window.

The local temperature profile of the troposphere is set by the lapse rate, which depends on the surface temperature, the relative humidity and the convection from the surface. The stratosphere is heated mainly by the absorption of UV solar flux by ozone and cools by LWIR emission from  $\text{CO}_2$  and ozone. The local solar heating changes on a daily and a seasonal time scale. The downward flux from the LWIR emission in the stratosphere and upper troposphere are absorbed in the lower troposphere and do not reach the surface. The local temperature of an air parcel in the stratosphere depends on the local flux balance. There is no 'equilibrium state' that can be perturbed by a change in  $\text{CO}_2$  concentration. The OLR flux defines a set of cooling rates for various levels in the atmosphere. Any change in the LWIR flux from a change in atmospheric  $\text{CO}_2$  concentration defines a change in these cooling rates that has to be integrated over time to determine the change in enthalpy of the local air parcels in the atmosphere.

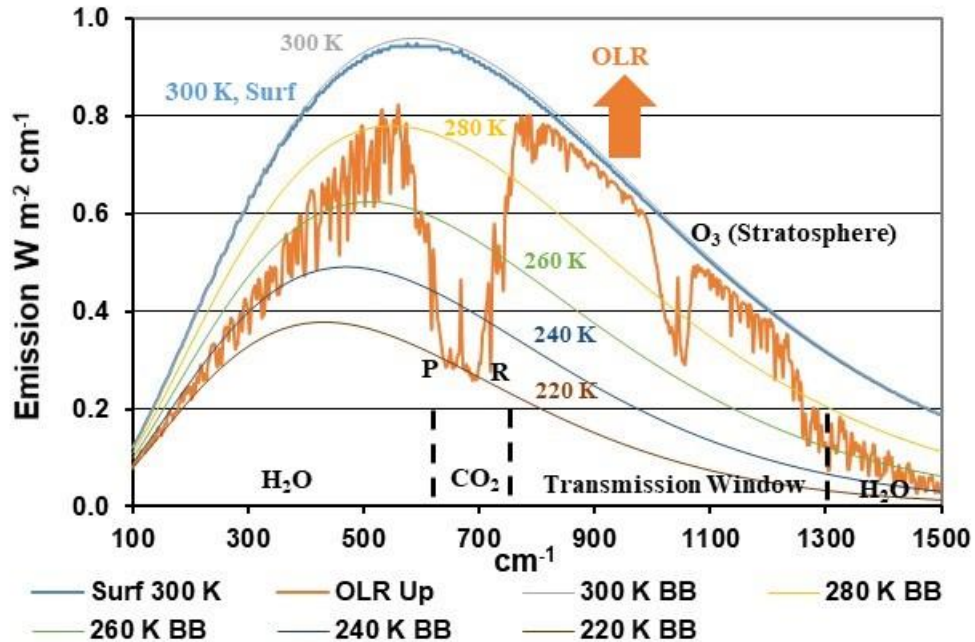


Figure 4: Spectral distribution of the OLR flux to surface for a 300 K surface temperature. The principal spectral features are indicated (MODTRAN calculation).

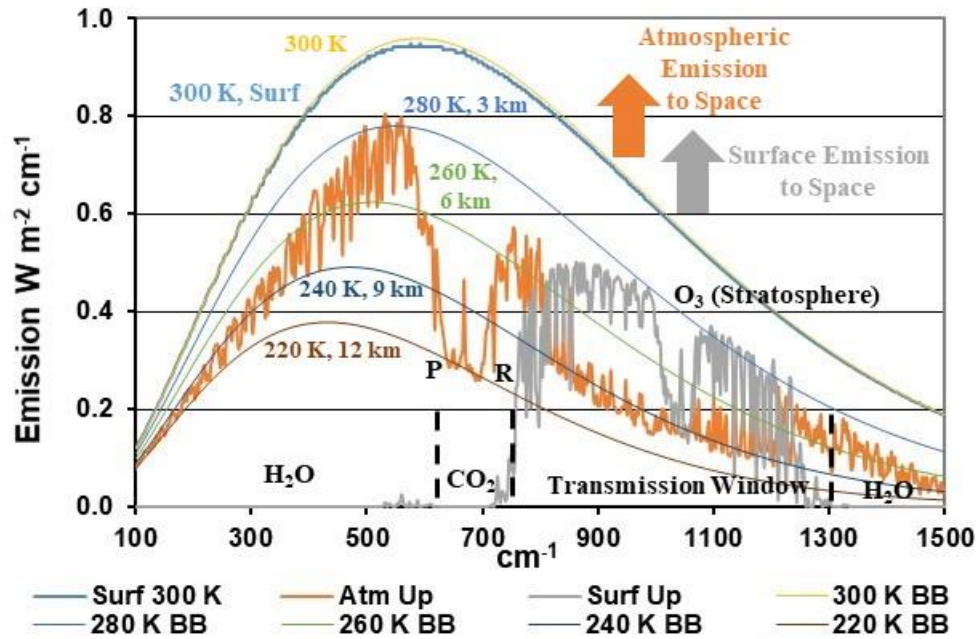


Figure 5: OLR to space, 300 K surface temperature showing the separate atmospheric and surface contributions to the 70 km level emission (MODTRAN calculation).

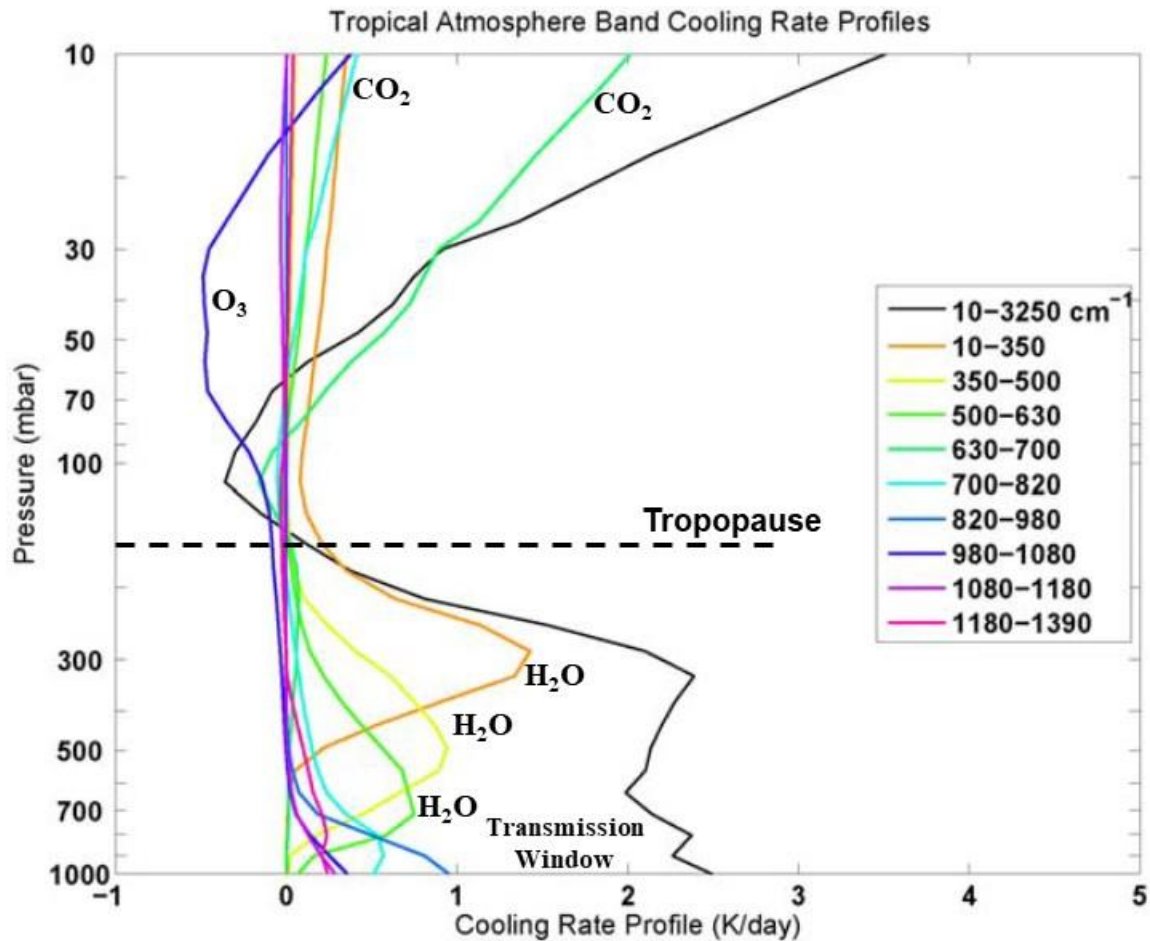
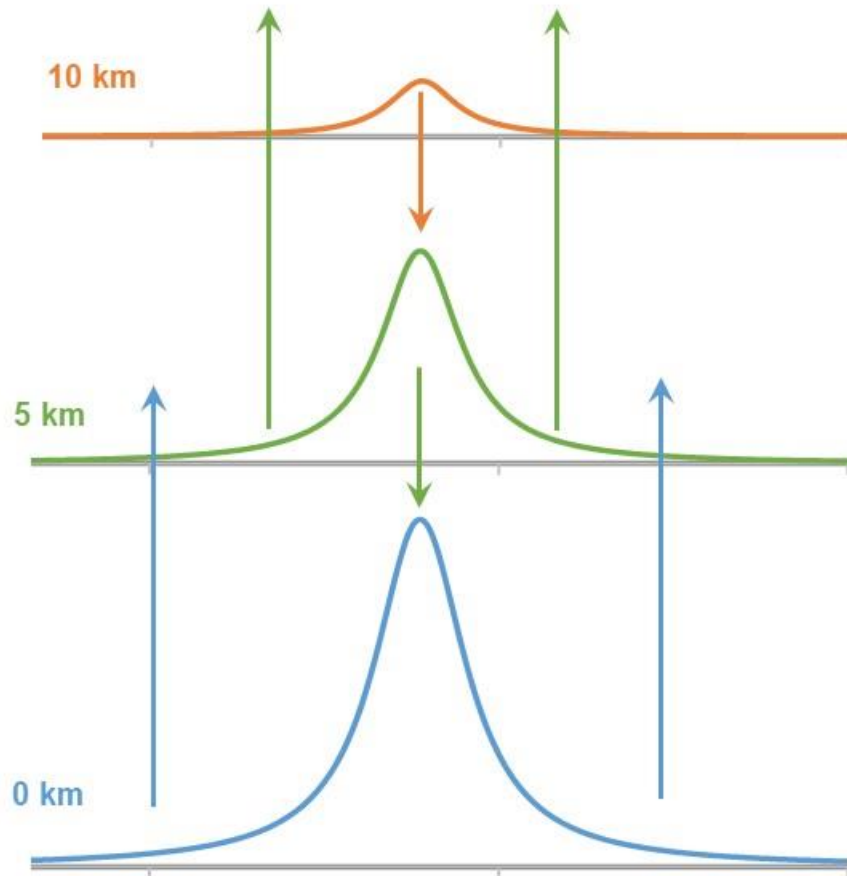


Figure 6: Total and band-averaged IR cooling rate profiles for the Tropical Model Atmosphere on a log-pressure scale [Feldman et al, 2008]

### Molecular Linewidth Effects

The LWIR absorption and emission in the atmosphere from H<sub>2</sub>O and CO<sub>2</sub> consists of thousands of lines each involving transitions between specific molecular rotation-vibration states. Through the troposphere and most of the stratosphere the molecular linewidth is determined by pressure broadening. This is the result of molecular collisions. Near the surface, within the main absorption bands the individual lines merge to form a quasi-continuous blackbody. The absorption and the molecular linewidths decrease as the pressure, temperature and the species concentration decrease with altitude. This means that the upward and downward LWIR flux through the atmosphere are not equivalent. Some of the upward flux from the wings of the broader lines below can pass through the gaps between the lines above. Conversely the downward flux from the narrower lines above is fully absorbed by the wider lines below. The change in linewidth with altitude is illustrated in Figure 7. This also means that all of the downward flux reaching the surface from within the main absorption bands is emitted from within the first 2 km layer above the surface. Almost half of this flux is emitted from within the first 100 m layer above the surface. It is this downward flux that provides the photons for the surface exchange energy. The cumulative

downward flux from H<sub>2</sub>O and CO<sub>2</sub> vs. altitude is shown in Figure 8. Four cases are plotted for surface temperatures of 272 and 300 K each with relative humidities of 20 and 70%. The downward flux near the surface increases with temperature and humidity. Even for the lowest flux case, 272 K and 20% RH, 95% of the surface flux originates from within the first 2 km layer. This means that the downward flux to the surface is decoupled from the LWIR emission to space. The concept of radiative forcing is invalid. There is no equilibrium flux that can be perturbed by an increase in 'greenhouse gas' concentration.



**Figure 7: Transition from absorption-emission to free photon flux as the linewidth decreases with altitude. Single H<sub>2</sub>O line near 231 cm<sup>-1</sup>**

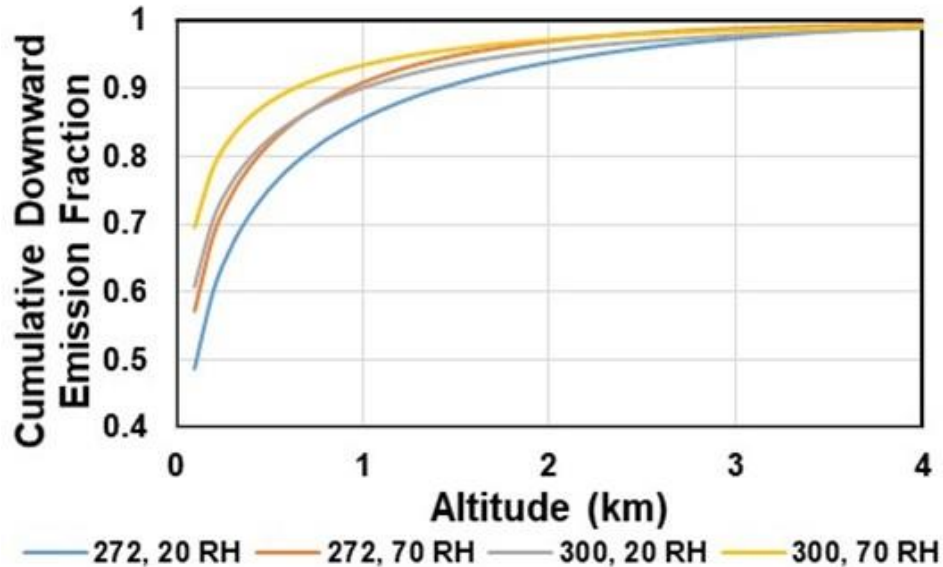


**Figure 8:** Cumulative fraction of the downward flux at the surface vs. altitude for surface temperatures of 272 and 300 K, each with 20 and 70% RH. Almost all of the downward flux reaching the surface originates from within the first 2 km layer. This is the lower tropospheric reservoir.

### The Coupling of the Downward LWIR Flux into the Surface Thermal Reservoirs

At the local surface, the solar flux is always changing on both a daily and a seasonal time scale. The peak solar flux with the sun overhead is approximately  $1000 \text{ W m}^{-2}$  and this corresponds to a blackbody emission temperature of about 94 C. During the day as the sun illuminates the surface, heat is stored below the surface and released over a range of time scales. In order to dissipate the heat from the surface there must be a time dependent thermal gradient. This of course follows from the Second Law of Thermodynamics. For evaporation, a humidity gradient is required, which usually includes a thermal gradient.

The land and ocean surfaces behave differently and must be considered separately. Over land, the incident solar flux, the net LWIR flux, the convection or sensible heat flux and the latent heat flux interact with a thin surface layer. The net LWIR cooling flux is insufficient to dissipate the absorbed solar flux. The surface heating produces a thermal gradient both with the air layer above and the subsurface layers below. The surface-air gradient drives the convection or sensible heat flux. The subsurface thermal gradient conducts heat into the first 0.5 meter layer of the ground. Later in the day this thermal gradient reverses and the stored heat is released back into the troposphere. The thermal gradients are reduced by evaporation if the land surface is moist. An important consideration in setting the land surface temperature is the night time convection transition temperature at which the surface and surface air temperatures equalize. Convection then essentially stops and the surface continues to cool more slowly by net LWIR emission. The convection transition temperature is reset each day by the local weather conditions. This is discussed in more detail by Clark [2019a].

The ocean surface is almost transparent to the solar flux. Approximately 90% of the solar flux is absorbed within the first 10 m layer. The surface-air temperature gradient is quite small, usually less than 2 K. The excess absorbed solar heat is removed through a combination of net LWIR flux emission and wind driven evaporation. The penetration depth of the LWIR flux into the ocean surface is 100  $\mu\text{m}$  or less and the evaporation involves the removal of water molecules from a thin surface layer. These two processes combine to produce cooler water at the surface. This then sinks and is replaced by warmer water from below. This is a Rayleigh-Benard convection process, not simple diffusion. The upwelling warm water allows the wind driven ocean evaporation to continue at night. As the cooler water sinks, it carries with it the surface momentum or linear motion produced by the wind coupling at the surface. This establishes the subsurface ocean gyre currents.

It is also important to understand that the surface energy transfer processes are part of the tropospheric heat engine [Clark, 2013a, b; Oke, 2016]. This removes heat from the surface and transfers it to higher altitudes by convection. From here it is radiated back to space. This heat engine has some unusual properties. It operates at low temperatures and pressures. This means that the LWIR flux cannot be described simply in terms of blackbody radiation. Instead, a high spectral and spatial resolution radiative transfer analysis is required. Most of the heat is removed from the surface by moist convection. This is a mass transport process that is coupled both to the earth's gravitational field and the earth's axial rotation or angular momentum. As a warm air parcel ascends from the surface it must expand and cool as it performs mechanical work to overcome the gravitational potential. This establishes the tropospheric temperature profile or lapse rate. The cooling produced by convection is usually much larger than that produced by net LWIR emission. The LWIR flux cannot be separated from the convection and analyzed independently. The local LWIR flux is emitted at the local air temperature. The coupling of the ascending air parcel to the rotation of the earth establishes the basic Hadley, Ferrell and Polar convective cell structure which in turn drives the trade winds and the ocean gyre circulation. The earth's weather patterns are determined mainly by the thermodynamic and fluid dynamic properties of the tropospheric heat engine, not the LWIR flux. The earth's climate is the long term (30 year) average of these weather patterns.

The land and especially the oceans are the hot reservoirs ('boilers') of the tropospheric heat engine. The troposphere divides naturally into two independent thermal reservoirs [Clark, 2019b; 2019c; 2013a; 2013b]. Almost all of the downward LWIR flux reaching the surface originates from within the first 2 km layer that forms the lower tropospheric reservoir. The LWIR emission to space originates mainly from the upper tropospheric reservoir that extends from 2 km to the tropopause. This acts as the cold reservoir of the heat engine. The heat lost by LWIR emission to space is replaced by convection from below. Above the tropopause, the stratosphere forms a third independent thermal reservoir. The main heat source here is absorption of the UV solar flux by ozone and the cooling is dominated by LWIR emission from  $\text{CO}_2$ . The downward LWIR flux to the surface and the outgoing LWIR radiation to space are decoupled by the molecular line broadening effects. These energy transfer processes are illustrated in Figure 9.

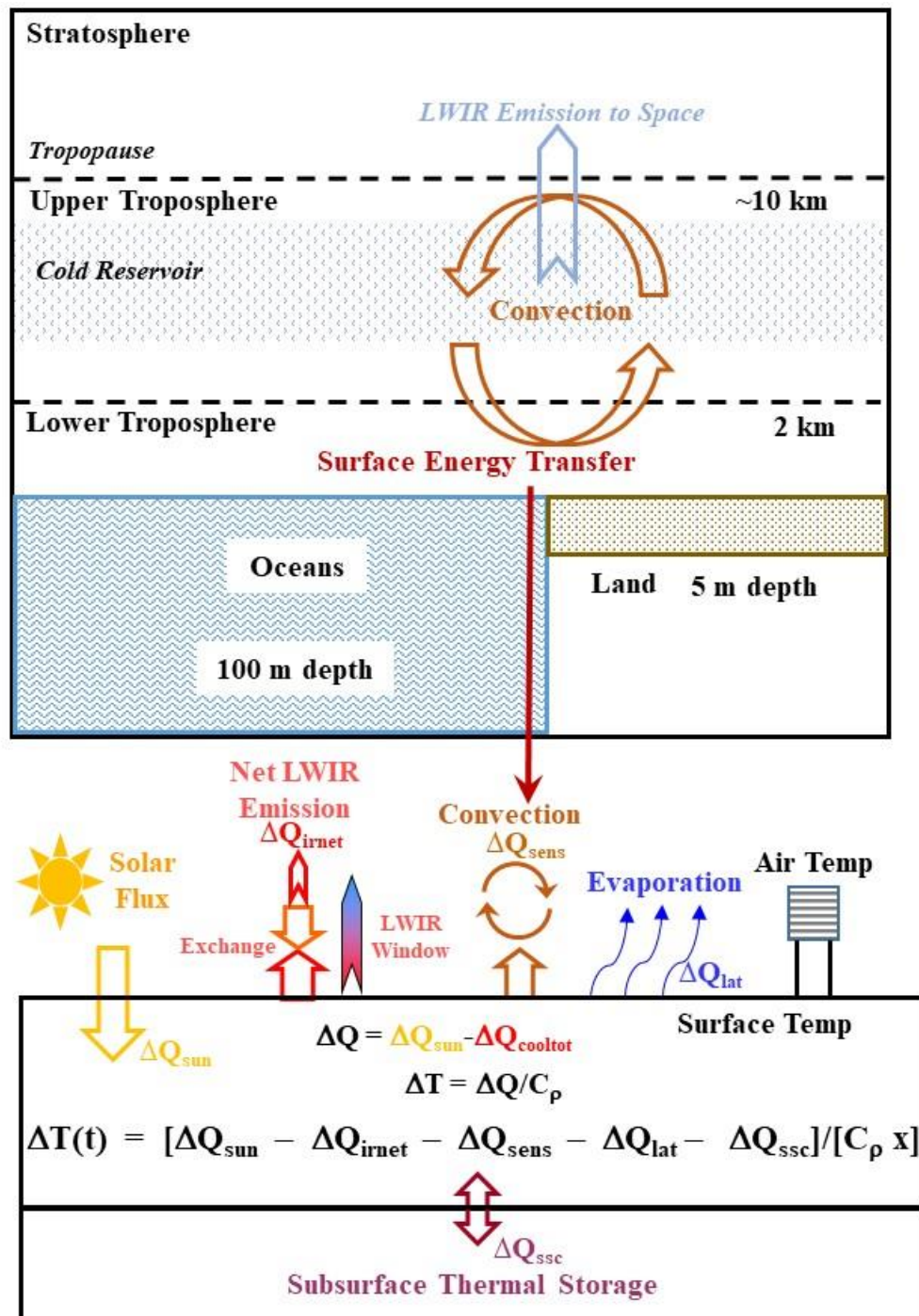


**Figure 9: Thermal reservoirs, surface energy transfer and thermal storage (schematic). The surface is heated by the sun and cooled by a combination of net LWIR emission, convection and evaporation. Heat is stored below the surface and released over a range of time scales. There is no ‘equilibrium average temperature’.**

Historically, the weather station temperature record for the US consisted of the minimum and maximum MSAT recorded using Six’s thermometer. These two temperatures record different

energy transfer processes. The minimum MSAT generally occurs near dawn. At this time, the surface air layer and the ground are usually at similar temperatures and the minimum MSAT is approximately that of the bulk surface air temperature of the local weather system that is passing through. The maximum MSAT is generally recorded in the early afternoon after the peak solar flux at local noon. It is the air temperature produced by the convective mixing of the warm air rising from the surface as it interacts with the cooler air at the MSAT thermometer level. The increase in temperature from the minimum to the maximum is a combined measure of convective mixing, solar flux, cloud cover and surface moisture/precipitation. This means that the energy transfer information is contained in the minimum MSAT and the delta or (max – min) MSAT. In order to calculate an average daily MSAT temperature, the minimum and maximum MSATs have to be determined first [Clark, 2019a].

When the time dependence is explicitly included in the surface temperature calculation, there is another parameter that also needs to be considered. This is the time delay or phase between the peak solar flux and the surface temperature response. This is a well-known property of non-equilibrium energy storage systems. The phase shift in the land subsurface temperature response was described by Fourier in 1827. The diurnal phase shift may reach 2 or more hours. However, this is not normally measured as part of the temperature record and would not be recorded by Six's thermometer. There is also a seasonal phase shift that may reach 6 to 8 weeks. This can only come from the ocean thermal response because the heat capacity of the land thermal reservoir is too small. This phase shift can be observed by weather stations that are long distances from the ocean, such as Sioux Falls, SD. This provides clear evidence of the transport of ocean surface temperature information over long distances by weather systems that are formed over the oceans. The transport mechanism is through the convection transition temperature [Clark, 2019a].

Over the last 200 years, the atmospheric concentration of CO<sub>2</sub> has increased by 120 ppm from 280 to 400 ppm. This has produced an increase in downward long wave IR flux at the earth's surface of approximately 2 W m<sup>-2</sup>. When this increase in flux is added to the dynamic surface energy flux balance, the change in surface temperature is too small to measure. Over land, the increase in LWIR flux is coupled into the moist convection and the subsurface thermal reservoir enthalpy. Over the oceans, the increase in flux is mixed within the first 100 μm surface layer with the much larger and more variable wind driven evaporation term.

The concept of radiative forcing has no basis in physical reality. Small changes in LWIR flux at the tropopause cannot couple into the surface thermal reservoirs and cause any measurable change in surface temperature

## References

Clark, R. 2019a, 'A Dynamic Coupled Thermal Reservoir Approach to Atmospheric Energy Transfer Part III: The surface Temperature', Ventura Photonics Monograph, VPM 004.1, Thousand Oaks, CA, May 2019

[http://venturaphotonics.com/files/CoupledThermalReservoir\\_Part\\_III\\_Surface\\_Temperature.pdf](http://venturaphotonics.com/files/CoupledThermalReservoir_Part_III_Surface_Temperature.pdf)

Clark, R. 2019b, 'A Dynamic Coupled Thermal Reservoir Approach to Atmospheric Energy Transfer Part IV: The Null Hypothesis for CO<sub>2</sub>' Ventura Photonics Monograph, VPM 005.1, Thousand Oaks, CA, May 2019

[http://venturaphotonics.com/files/CoupledThermalReservoir\\_Part\\_IV\\_The\\_Null\\_Hypothesis.pdf](http://venturaphotonics.com/files/CoupledThermalReservoir_Part_IV_The_Null_Hypothesis.pdf)

Clark, R. 2019c, 'A Dynamic Coupled Thermal Reservoir Approach to Atmospheric Energy Transfer Part V: Summary', Ventura Photonics Monograph, VPM 006, Thousand Oaks, CA, May 2019

[http://venturaphotonics.com/files/50\\_Years\\_of\\_Climate\\_Fraud.pdf](http://venturaphotonics.com/files/50_Years_of_Climate_Fraud.pdf)

Clark, R. 2019d, 'The Greenhouse Effect', Ventura Photonics Monograph, VPM 003.2, Thousand Oaks, CA, May 2019

[http://venturaphotonics.com/files/The\\_Greenhouse\\_Effect.pdf](http://venturaphotonics.com/files/The_Greenhouse_Effect.pdf)

Clark, R., 2013a, *Energy and Environment* **24**(3, 4) 319-340 (2013), 'A dynamic coupled thermal reservoir approach to atmospheric energy transfer Part I: Concepts'

[http://venturaphotonics.com/files/CoupledThermalReservoir\\_Part\\_I\\_E\\_EDraft.pdf](http://venturaphotonics.com/files/CoupledThermalReservoir_Part_I_E_EDraft.pdf)

Clark, R., 2013b, *Energy and Environment* **24**(3, 4) 341-359 (2013) 'A dynamic coupled thermal reservoir approach to atmospheric energy transfer Part II: Applications'

[http://venturaphotonics.com/files/CoupledThermalReservoir\\_Part\\_II\\_E\\_EDraft.pdf](http://venturaphotonics.com/files/CoupledThermalReservoir_Part_II_E_EDraft.pdf)

Feldman D.R., Liou K.N., Shia R.L. and Yung Y.L., *J. Geophys. Res.* **113** D1118 pp1-14 (2008), 'On the information content of the thermal IR cooling rate profile from satellite instrument measurements'

Fourier, B. J. B.; *Mem. R. Sci. Inst.*, (7) 527-604 (1827), 'Memoire sur les temperatures du globe terrestre et des espaces planetaires'

Hansen, J. et al, (45 authors), *J. Geophys. Research* **110** D18104 1-45 (2005) 'Efficacy of climate forcings' <http://pubs.giss.nasa.gov/abs/ha01110v.html>

Hansen, J.; D. Johnson, A. Lacis, S. Lebedeff, P. Lee, D. Rind and G. Russell *Science* **213** 957-956 (1981), 'Climate impact of increasing carbon dioxide'

Harde, H., *Int. J. Atmos. Sci.* 9251034 (2017), 'Radiation Transfer Calculations and Assessment of Global Warming by CO<sub>2</sub>', <https://doi.org/10.1155/2017/9251034>

IPCC, 2013: *Climate Change 2013: The Physical Science Basis. Contribution of Working Group I to the Fifth Assessment Report of the Intergovernmental Panel on Climate Change* Chapter 8 'Radiative Forcing' [Stocker, T.F., D. Qin, G.-K. Plattner, M. Tignor, S.K. Allen, J. Boschung, A. Nauels, Y. Xia, V. Bex and P.M. Midgley (eds.)]. Cambridge University Press, Cambridge, United Kingdom and New York, NY, USA, 1535 pp, doi:10.1017/CBO9781107415324.

<http://www.climatechange2013.org/report/full-report/>

Koll, D. D. B and T. W. Cronin., *PNAS*, [www.PNAS.Org/Cgi/doi/10.1073/pnas.1809868115](http://www.PNAS.Org/Cgi/doi/10.1073/pnas.1809868115) pp. 1-6 (2018), 'Earth's outgoing longwave radiation linear due to H<sub>2</sub>O greenhouse effect'.

MODTRAN 2018, <http://forecast.uchicago.edu/Projects/modtran.orig.html>

Oke T. R., WMO/TD-No. 1250, World Meteorological Association, 2006, 'Initial guidance to obtain representative meteorological observations at urban sites'